Object Discrimination and Optical Performance of a Real-Time 2-5 μm Hyperspectral Imager

Mark Dombrowski[a], Rachael Dombrowski[a], Brian Catanzaro[b], Eric Hillenbrand[c]

[a] Surface Optics Corporation[1]
[b] CFE Services, 5147 Pacifica Dr., San Diego, CA 92109
[c] Naval Surface Warfare Center, Crane Division

ABSTRACT

Hyperspectral imaging in the 2-5 um band has held interest for applications in detection and discrimination of objects of interest. Real time instrumentation is particularly powerful as a tool for characterization and field measurement. A compact, real-time, refractive MWIR hyperspectral imaging instrument has been designed and tested. The system has been designed for cryogenic operation to improve signal to noise ratio, reduce background noise, and enable real-time hyperspectral video processing. The system is a a 2-5 μm 32-band hyperspectral imager capable of collecting and processing complete hyperspectral image cubes at 15 cubes-per-second. Details of the system and object discrimination using this system are presented.
.

Keywords: Hyperspectral imaging, MWIR, Slit-based, Prism based, Cryogenic, HgCdTe

1. REAL-TIME HYPERSPECTRAL IMAGING

Real-time imaging over broad bands in the electromagnetic spectrum from the ultraviolet (UV) through the infrared (IR) has been a staple in the areas of remote sensing, surveillance, target detection and tracking, search and homing devices, spectrally tailored coating development, nondestructive inspection, and noninvasive diagnosis. Improvements are being made in these techniques all the time, with increased resolution, higher sensitivity, and greater information throughput being the benefit. Instrumentation developed at Surface Optics has been used to distinguish objects based on their spectral signature in a number of applications. These include: revealing camouflaged military targets, friend-foe identification based on subtle coloring of personnel uniforms, and identification of healthy and stressed vegetation based on changes in the Chlorophyll edge. [1,2]

2. SYSTEM ARCHITECTURE

The goals for a MWIR Hyperspectral Imager (MWIR HSI) development at Surface Optics include:

- Operation over the MWIR spectrum: 2 – 5 μm
- Real time video data collection and processing: 15 hypercubes/sec
- Relatively rich spectrum: 32 bands
- Field deployable system

[1] Correspondence - Email: markd@surfaceoptics.com; Telephone: 858-675-7404

Algorithms and Technologies for Multispectral, Hyperspectral, and Ultraspectral Imagery XII, edited by Sylvia S. Shen, Paul E. Lewis, Proc. of SPIE Vol. 6233, 62330Q, (2006) · 0277-786X/06/$15 · doi: 10.1117/12.665906

Figure 1 shows the assembled system and the system without its enclosure under test in the lab. Note the compact size of the instrument (23" x 9" x 7").

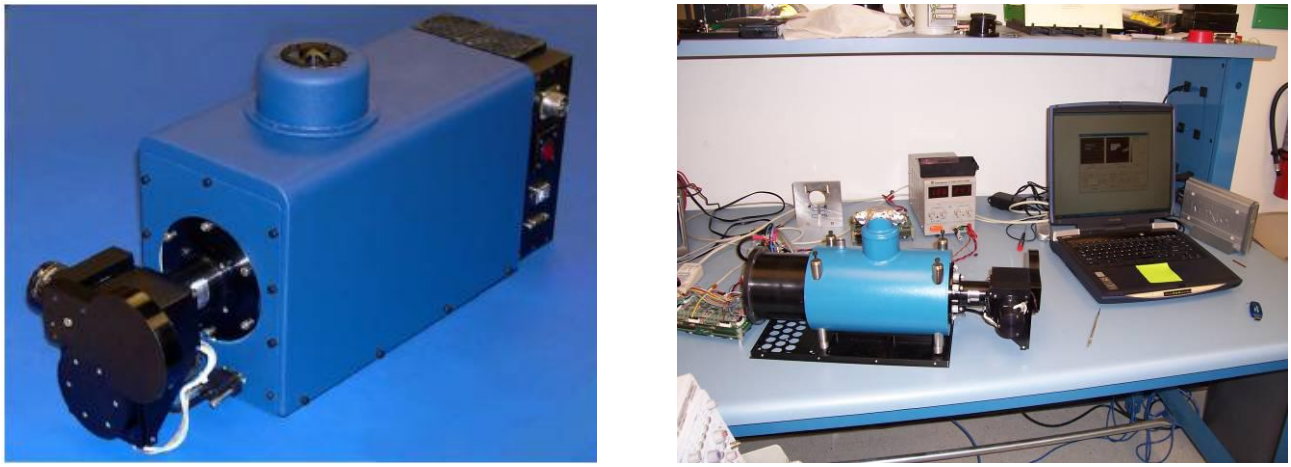

Figure 1: MWIR HSI fully assembled (left) and under test in the lab (right)

In order to achieve these goals, a system was designed around a slit-based optical system, with a prismatic dispersion element, passive athermalization, and a compact dewar (see Figure 2). The slit-based system produces an image in one direction and spectral bands in the direction orthogonal to the slit. A scan mirror translates the image across the slit to provide a full frame hyperspectral image. Dispersion is provided by a multi-element prism. The entire system is cooled to cryogenic temperatures to reduce background noise which appears broadband on the detector.

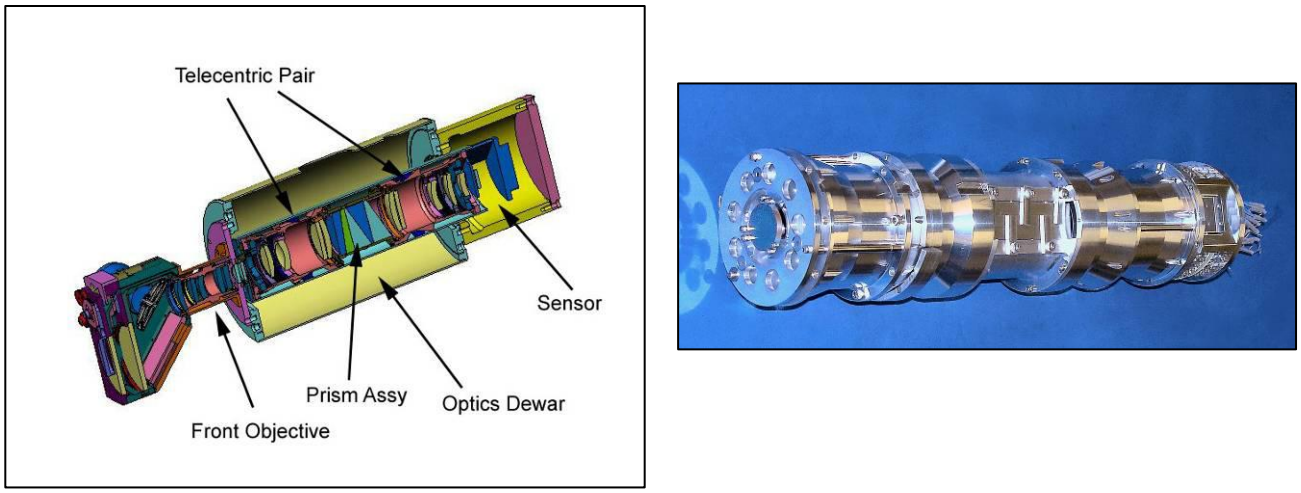

Figure 2: MWIR HIS Optical Model (left) and completed spectrometer assembly (right)

A key element in the system is the focal plane array (FPA). The hypercube consists of 256 x 256 pixels by 32 wavebands at 15 hypercubes/sec. The relatively narrow spectral bandwidth of each waveband results in a very low irradiance on the pixels of the FPA – approximately 3% of a broadband MWIR scene - significantly less in wavelengths around 3 μm. This situation prevents the use of room temperature microbolometer arrays. Figure 3 shows the comparison of the SNR of a 300K blackbody scene viewed at various wavebands. For this application, the SNR for the

cooled FPA is 100X to 1000X that of the uncooled technology.[2] In addition, a single detector technology that can be used for SWIR and LWIR wavebands inspired the use of a HgCdTe FPA.

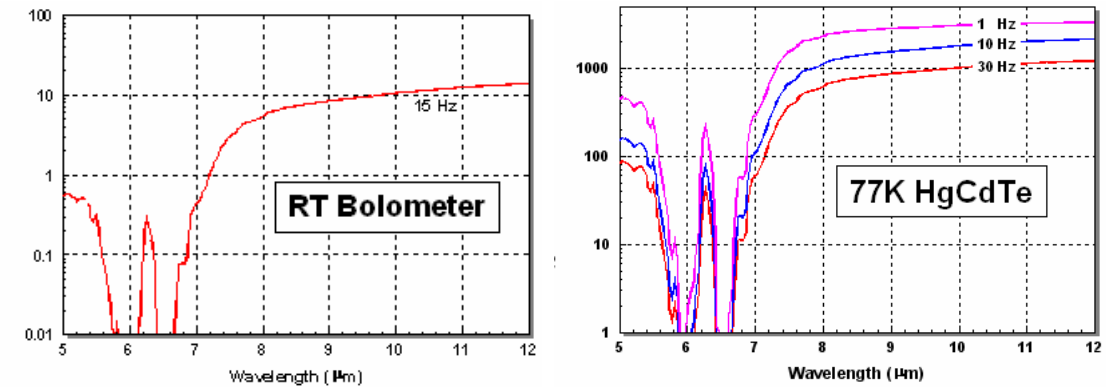

Figure 3: SNR of RT Bolometer and 77k HgCdTe FPA's

Some of the major design challenges for this system include:

- Optical design of an F/1.75 achromatic, infinite conjugate
- Achieving optical performance (passive athermalization, wavefront error, dispersion) at 77 K
- Cryogenic opto-mechanical design

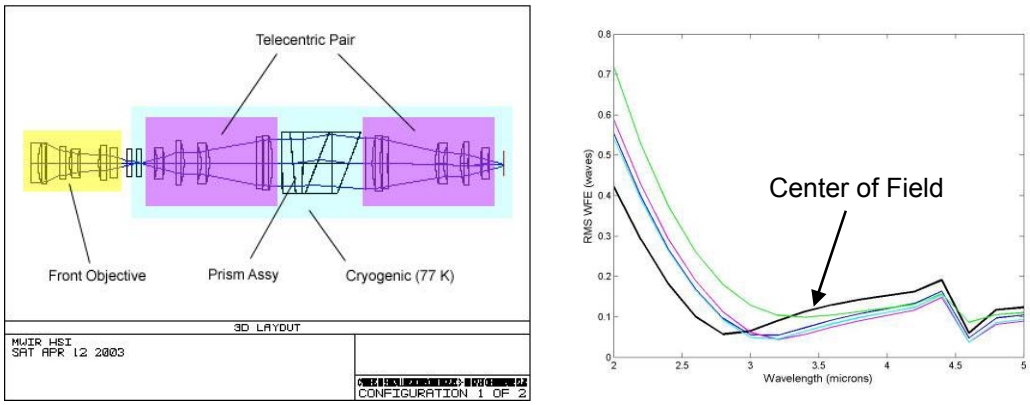

Figure 4: Optical Layout and Wavefront Error

The authors have reported on some of these challenges previously [3]. For summary purposes, the optical layout and wavefront error (WFE) of the system are shown in Figure 4.

3. MWIR HSI STATUS

The SWIR/MWIR HSI has been fully integrated, tested, and delivered to an end-user. The system has demonstrated good spatial and spectral resolution and low-noise performance at the full 15 cubes-per-second.

3.1 CRYOGENIC PRISM HOUSING

[2] F/1 optics, Frame Rate = Cubes/sec, 25 C Sunlit grass field, 100 m from Imager

The prism housing is a critical component that provides the structural support, orientation, and spacing for the prism elements. The materials used in the prism (germanium, calcium fluoride, zinc selenide) must be protected from undue compressive forces when the system cools down. In addition, the wavefront error requirements of the system are near diffraction limit. Given the number of elements in the system, the maximum allowable contribution from each element from cryogenic distortion is quite small ($WFE_{element} < \lambda/40$ RMS). For these reasons, special attention was paid to the design of the prism holder.

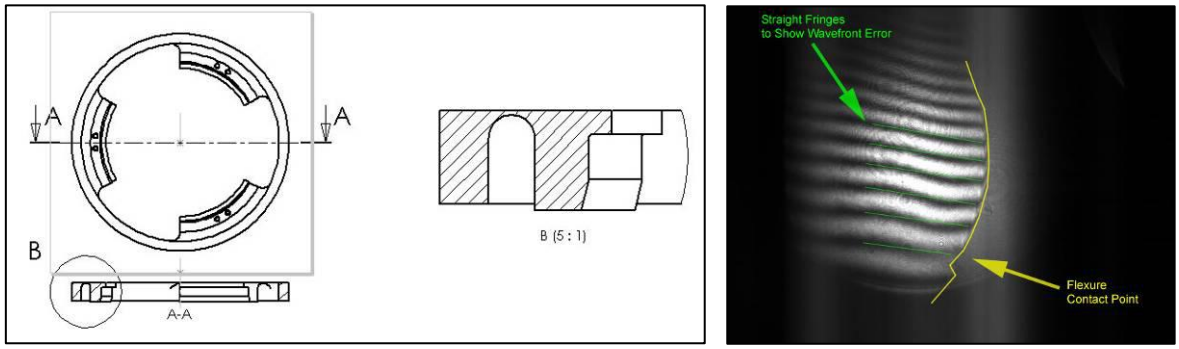

Figure 5: Lens Mount and Results for Stress Induced in Test Optic

In a previous publication [3], the opto-mechanical design of the lens holders was reviewed. These holders were designed with single blade flexures in a radial configuration (see Figure 5). Using shims, the stress on a test optic was measured and the peak-to-valley (PV) WFE was evaluated. Using this data as the criteria for maximum stress, a prism holder was designed to limit the stress on the prism elements below a critical value of 2 MPa.

Figure 6: Prism Assembly

The prism housing consisted of a load spreading bar suspended by flat springs that held the prism in a clam-shell cross-section tube (see Figure 6). The clam-shell only contacts the prisms along the bottom 30% of their circumference, removing the radial and hoop stress from the aluminum housing. Flat springs are used to provide a pre-load on a load spreading bar on the top of the prisms. The pre-load can be designed to hold the prisms with enough load to keep them from moving under 10 or more G's of acceleration without causing stresses that would affect the optical quality of the prisms.

3.2 ROOM TEMPERATURE OPTICAL TESTING

The MWIR HSI optical system has 15 elements in the cryogenic section. With this many elements, it is prudent to test sub-sections of the optical system. The optical system can be separated into three (3) functional blocks: two infinite conjugate lenses and a prismatic disperser. A single infinite conjugate was tested both at room temperature and at

cryogenic temperature [3] and the performance was measured as diffraction limited. More recent tests include: test of infinite conjugate pair and line spread function tests.

4. ROOM TEMPERATURE HYPERSPECTRAL CUBES

Hyperspectral data was collected at room temperature to demonstrate spatial and spectral resolution. The system was configured with room temperature housings and a bolometer. Significant improvement in sensitivity and SNR resulted when the system was cooled and the HgCdTe FPA was used (see the next section). Spatial resolution was demonstrated using a USAF Resolution target chrome pattern on a zinc selenide substrate. Spectral resolution was demonstrated using plastic films.

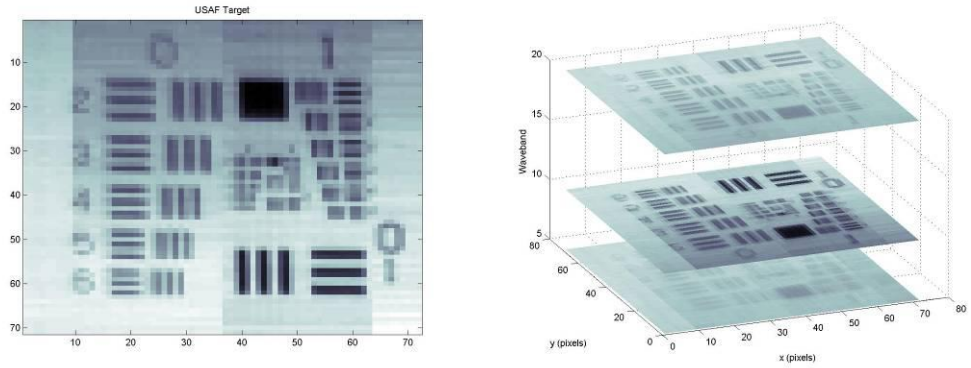

Figure 7: Hyperspectral Image of USAF Resolution Target

Figure 7 shows a hypercube for the USAF Resolution target. On the left is the image from a single spectral band demonstrating single pixel resolution. On the right, slices of the hypercube are shown. Images from three (3) of the wavebands are shown.

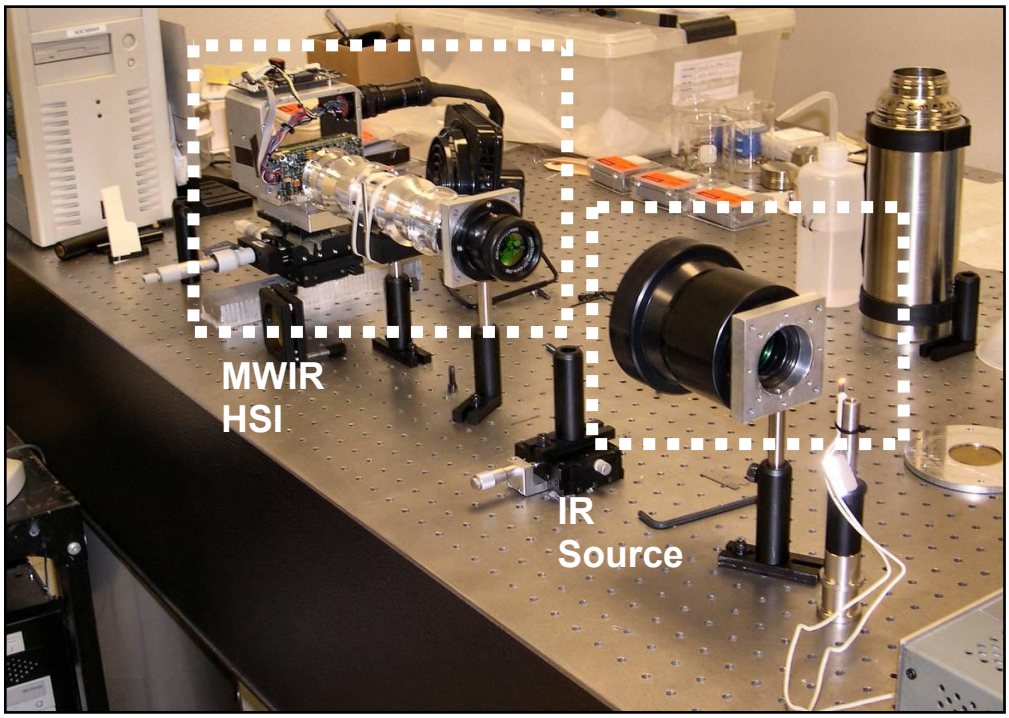

Figure 8: Hypercube Data Collection Test Setup

The MWIR HSI is not a thermal camera – it is a hyperspectral camera. As such, ideal objects to image have various spectral responses from 2 – 5 μm. The objects chosen were a series of plastic films were mounted on a single substrate. The films included varieties of kapton, polystyrene, and PET. In order to illuminate the sample, an infrared flashlight was constructed. A filament was used as the blackbody source. This filament was collimated with a fast infrared lens (Janos ASIO f = 100 mm). The system is shown in Figure 8.

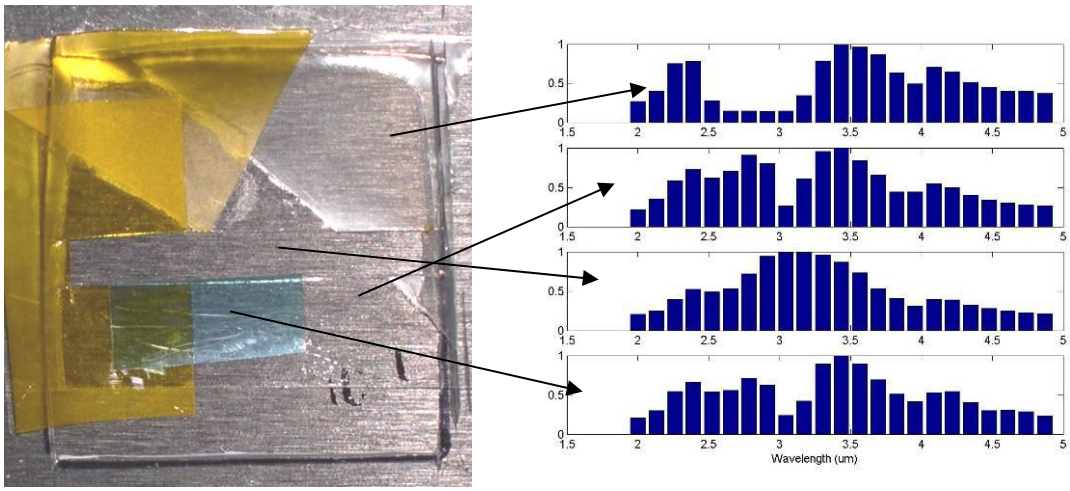

Figure 9: Plastic Film and Spectrum

The plastic film is shown in Figure 9 along with the spectrum from various portions of the image. The hypercube is shown in Figure 10 with several of the slices in the wavelength axis. The slices clearly indicate the various absorption spectrums of the different materials.

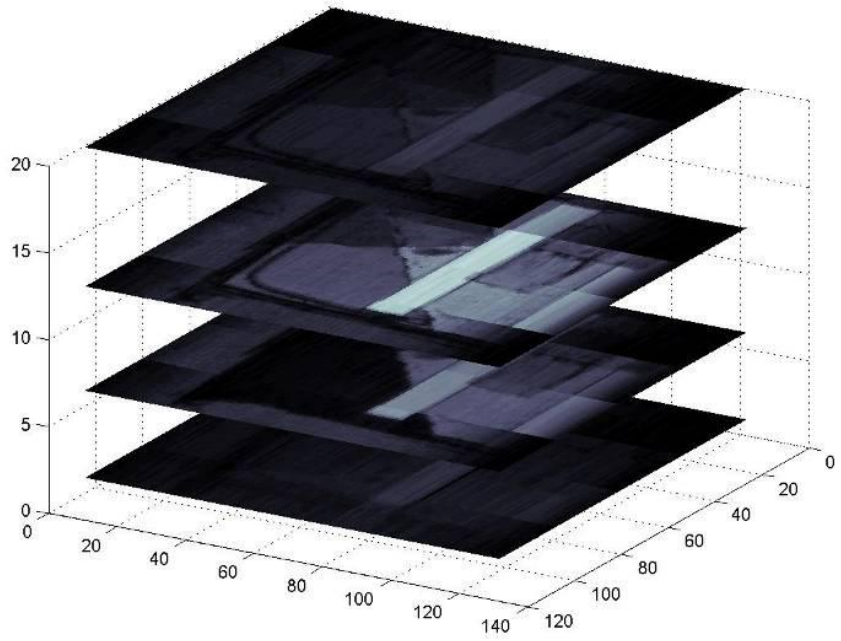

Figure 10: MWIR Hypercube for Plastic Film Sample

5. CRYOGENIC DATA

Uncalibrated data has been taken with the system operating at cryogenic temperatures, using a Rockwell HgCdTe focal plane array. The system exhibits very good sensitivity, even given the narrow (< 0.1 μm) bandwidth associated with each spectral line. Figure 11 shows two views of a person in a laboratory, one at 2.2 μm, and one at 4.7μm. A halogen lamp was used to produce enough 2.2 μm light to produce a usable image at this wavelength. Fluorescent room lights produce no output in this band. Note also that the two images were taken at slightly different times, between which the subject moved. Note, however, that these images were taken at the full temporal resolution of the system, 15 cubes-per-second.

Figure 11: Uncalibrated imagery at 2.2 μm (left) and 4.7 μm (right) taken at 15 cubes-per-second

Surface Optics' MIDIS-IV real time hyperspectral image processor has been integrated with the system; this processor performs real-time calibration and target detection using spectral discrimination algorithms. Figure 12 illustrates the Uncalibrated relative spectrum of the subject's shirt. Note the strong signal in the SWIR, and the H_20 and CO_2 absorption bands

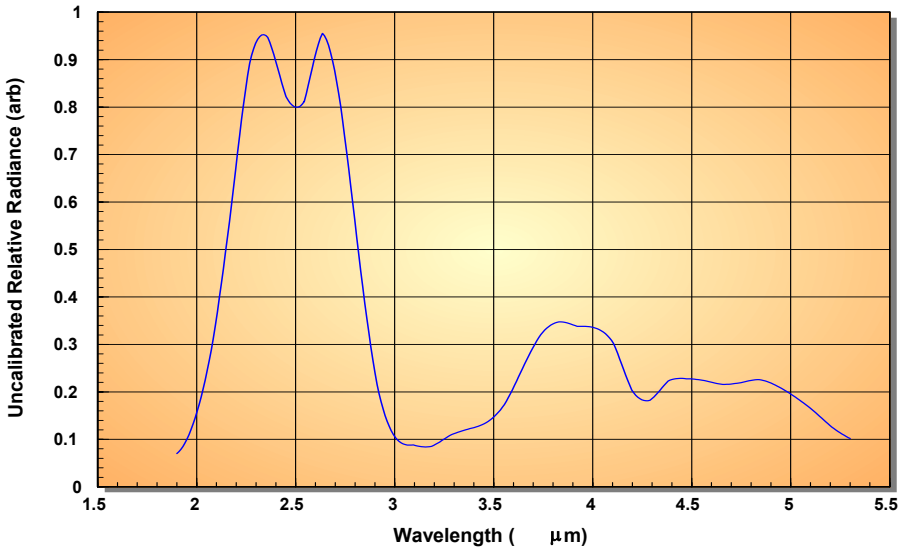

Figure 12: Uncalibrated spectrum from subject's shirt. Note absorption lines at 2.5 μm and 4.2 μm

5.1 REAL-TIME APPLICATIONS

A key feature of this SWIR/MWIR hyperspectral imager is the associated real-time processor, allowing the system to collect hyperspectral imagery, convert the raw imagery to spectro-radiometrically calibrated imagery, and identify objects or regions of interest based on spectral signatures. After the calibration section of the processor, two different processing functions are implemented. First, the processor applies three arbitrary response curves to each pixel's spectrum, integrating the result to produce three output images. Each of these images appear the same as if the scene had been viewed by a sensor with a spectral response the same as the applied response curve, allowing sensor emulation. By applying the three images to red, green, and blue display channels, a "true" color image results. True color here implies that the color imagery is based on each pixel's spectral radiance. False color images simply apply a color look-up to an inherently monochrome image. Figure 13 shows an example true color image, along with the response curves used to generate the image.

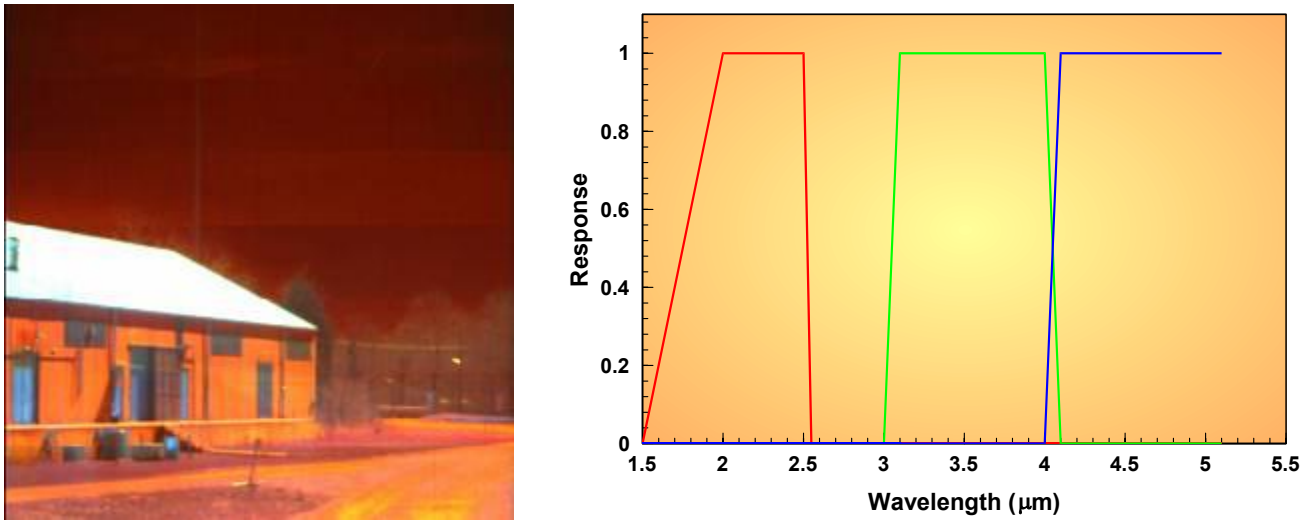

Figure 13: True color image produced by the MIDIS real-time processor and associated response curves

This image of an outside illuminated scene on a relatively cold day shows a great degree of spectral variability. As shown by the response curves, shortwave light (2.0 - 2.5 μm) is mapped to red, the low side of the midwave region (3.0 - 3.5 μm) maps to green, and the high side of the midwave region (4 .0 - 5.0 μm) maps to blue. The dark red sky in the above scene shows the SWIR scattered by the atmosphere, which also emits negligible light in the 3 - 5 μm range. The concrete sides of the building reflect strongly in the SWIR. Coupled with some reflected solar radiation in the 3-4 μm range and emitted energy, the building appears orange. The blue doors show very low SWIR reflectance and strong 4-5 μm radiance, providing the blue appearance. The cool plants around the road appear red due to reflected SWIR. Note the color gradations in the road, showing both temperature and emissivity differences.

The second function of the MIDIS real-time processor is to identify objects or regions in the scene of a given spectral distribution through a variety of spectral processing algorithms. Several tests were conducted to illustrate this capability. Gases posses unique absorption lines that allow identification, provided a temperature difference exists between the gas and the viewed background. Where the gas is cooler than the background, the gas shows an absorption feature; where the gas is warmer than the background, the gas shows an emission feature. When the gas and background are at the same temperature, absorption equals emission and no feature is visible. To demonstrate this capability, the system viewed a bottle of propane slowly releasing gas into the atmosphere. In the same scene, a small amount of ethanol slowly evaporated, providing an additional cloud. Figure 14 shows this scene at 2.1 μm, 2.4 μm, 3.4 μm, 3.5 μm, 3.6 μm, and after processing to reveal the gas plumes.

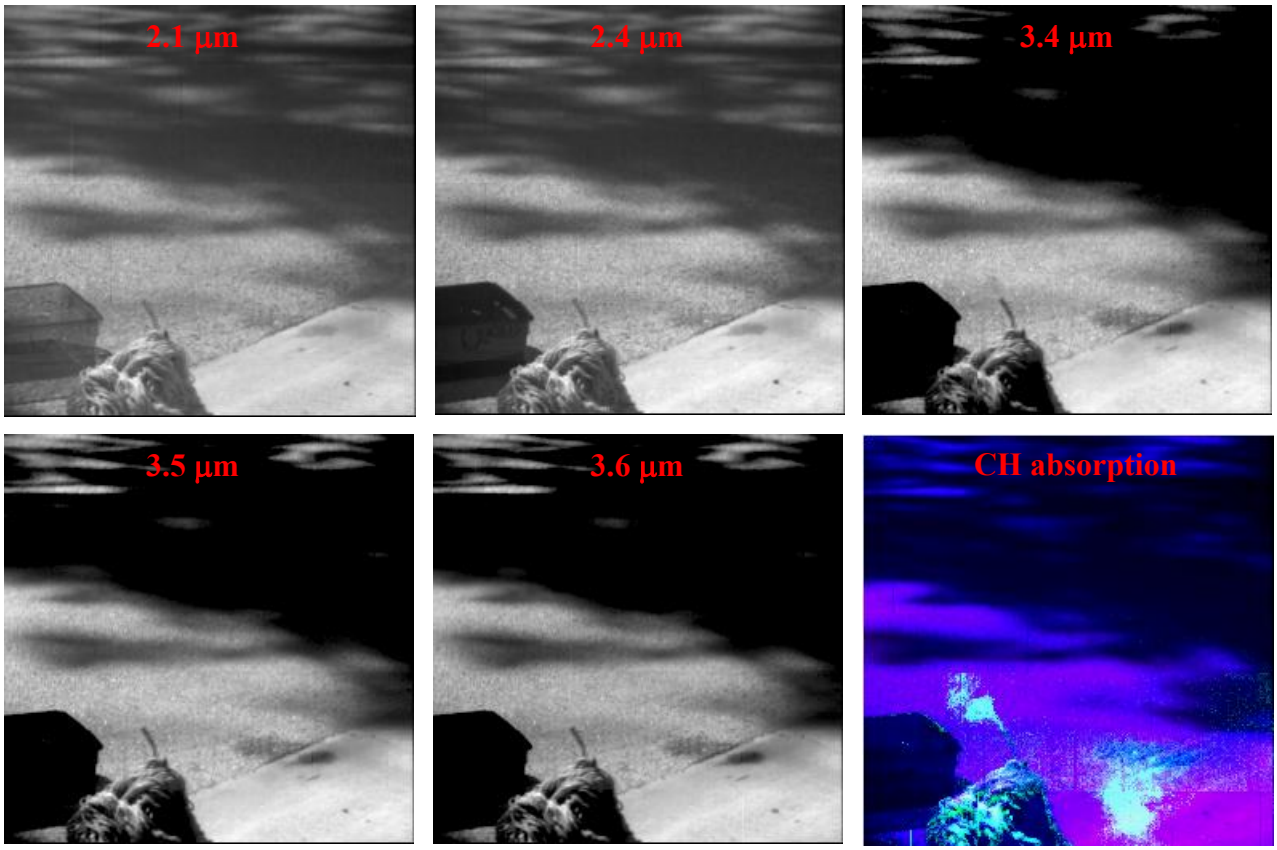

Figure 14: Several spectral bands show propane and ethanol absorption (3.4 µm & 3.5 µm) and processed plume

Obvious in the full-motion video, but not so obvious in the above images are the propane and ethanol plumes showing absorption at 3.4 µm and 3.5 µm from the C-H stretch in the hydrocarbons. Figure 15 shows the spectrum of a pixel near the propane plume relative to a pixel inside the plume. Note the absorption feature (shown as a positive peak) around 3.4 µm. The other spectral features are due to CO_2 around 4.4 µm and water around 2.5 - 3.0 µm. Looking carefully at the top of the torch and to the bottom left of the ethanol spill, a slight darkening at 3.4 µm and 3.5 µm

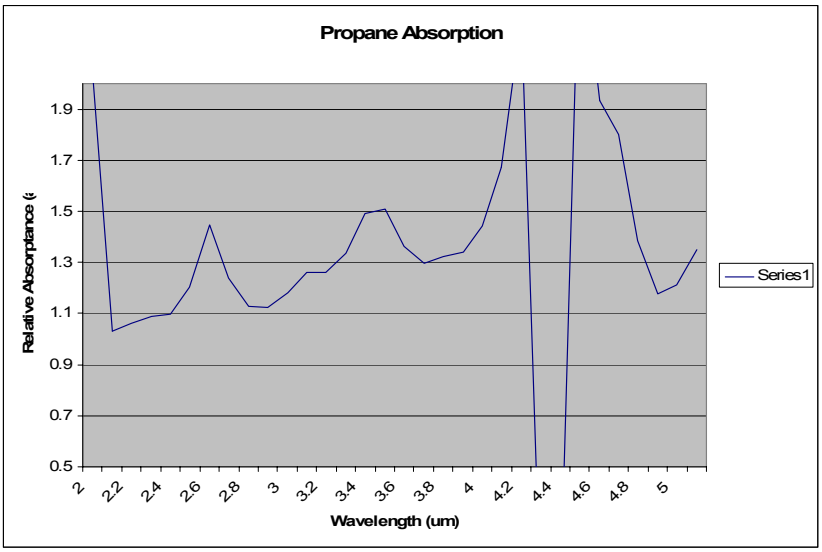

Figure 15: The C-H stretch absorption feature from Propane is clearly visible around 3.4 µm

reveals the plume locations. After processing by the MIDIS processor, however, the plumes are clearly visible. Note also that this data was taken during shifting wind conditions. The real-time video taken from the MIDIS processor clearly shows the development and dissipation of the plumes. Also not the changes in spectral characteristics of the plastic container at the bottom left of the image. At 2.1 μm it is transparent; at 2.4 μm it is mostly opaque, but careful inspection reveals writing at the top right corner. At 3.4 μm and beyond, the container is opaque and cold compared to the surrounding scene. Further inspection of the imagery reveals slightly less absorption from the propane and 3.5 μm compared to the ethanol. This slight difference ultimately allows differentiation of the two gases, although this processing has not yet been done.

Another example of hydrocarbon detection is shown in figure 16. In this figure, a light film of oil was smeared across a steel plate. At 2.2 μm, no hint of the oil is visible. In the middle of the C-H stretch at 3.4 μm, however, the oil and its thickness distribution across the plate is clearly visible. At 3.9 μm, only a slight darkening caused by a slight overall reduction in reflectance of the plate is noticeable. Also shown in the figure is uncalibrated radiance from two pixels in the images, on in the oil region, and one outside. The hydrocarbon absorption is clearly visible around 3.4 μm

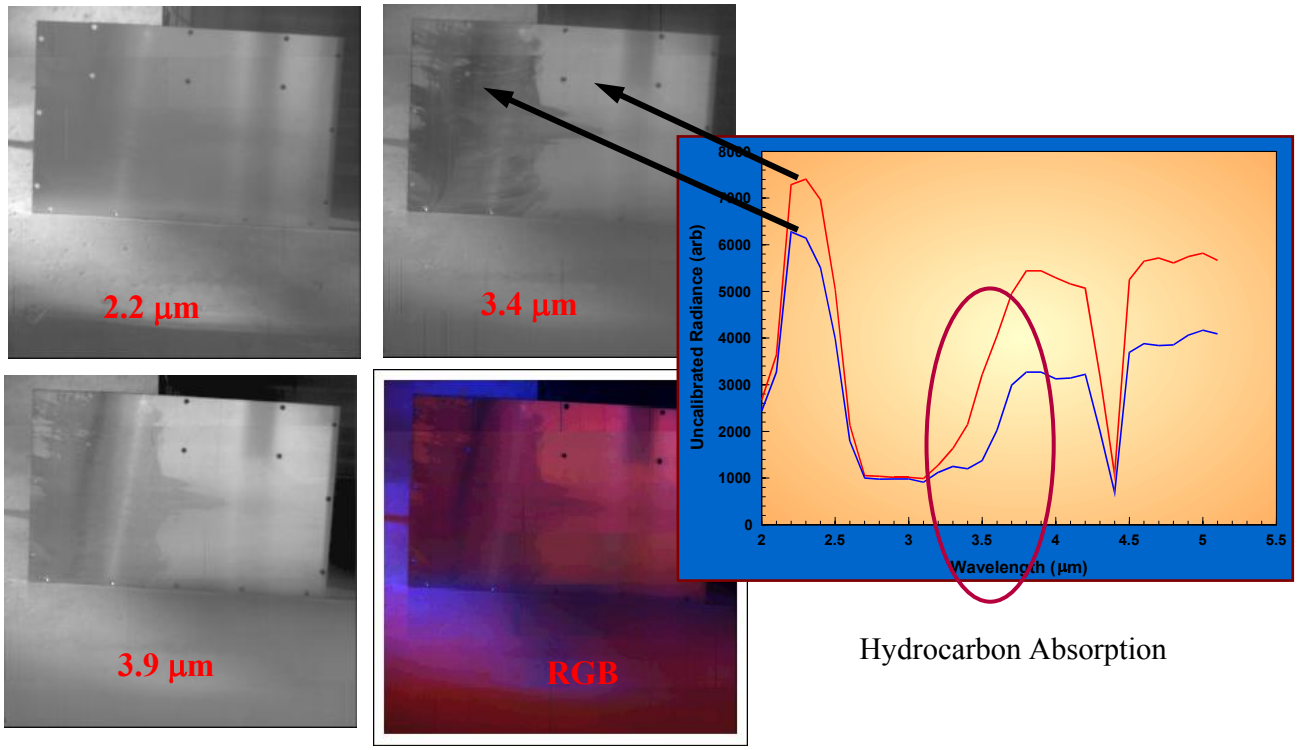

Figure 16: The C-H stretch absorption clearly shows oil film thickness at 3.4 μm

The CO_2 absorption feature at 4.4μm also reveals the presence of combustion through emission. At short ranges, the absorption of the atmosphere does not completely absorb the energy emitted in this band. At long range, of course, only a spike on the red side and a spike on the blue side of the absorption band, caused by pressure-broadening of the line, remain. Figure 17 shows an example of detection of CO_2 emission. In this image, the plume of warm air visible in the upper left corner is caused by a torch located out of the field of view of the imager. In the RGB image, the shadow of the torch, caused by SWIR sunlight, is visible in the middle left side of the image. Also note that the blue tint to the ground is caused by stronger SWIR radiance than MWIR radiance. The violet regions in the ground show areas were exhaust from the generator has heated up the ground, increasing the MWIR signature.

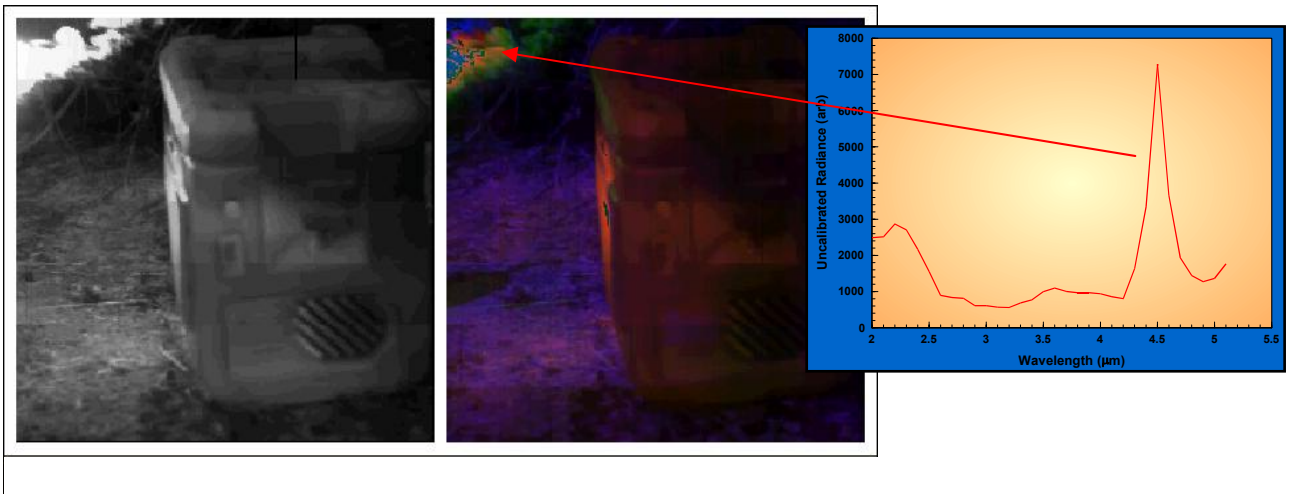

Figure 17: Warm CO_2 from a burning torch is clearly visible at 4.3 μm in the upper left corner of this video

One final application investigated with this real-time SWIR/MWIR hyperspectral imager and processor was personnel tracking. As shown in figure 11, skin exhibits a very low SWIR reflectance. Combined with relatively high emittance in the MWIR, this provides a strong spectral signature that can readily be tracked. Figure 18 illustrates this capability.

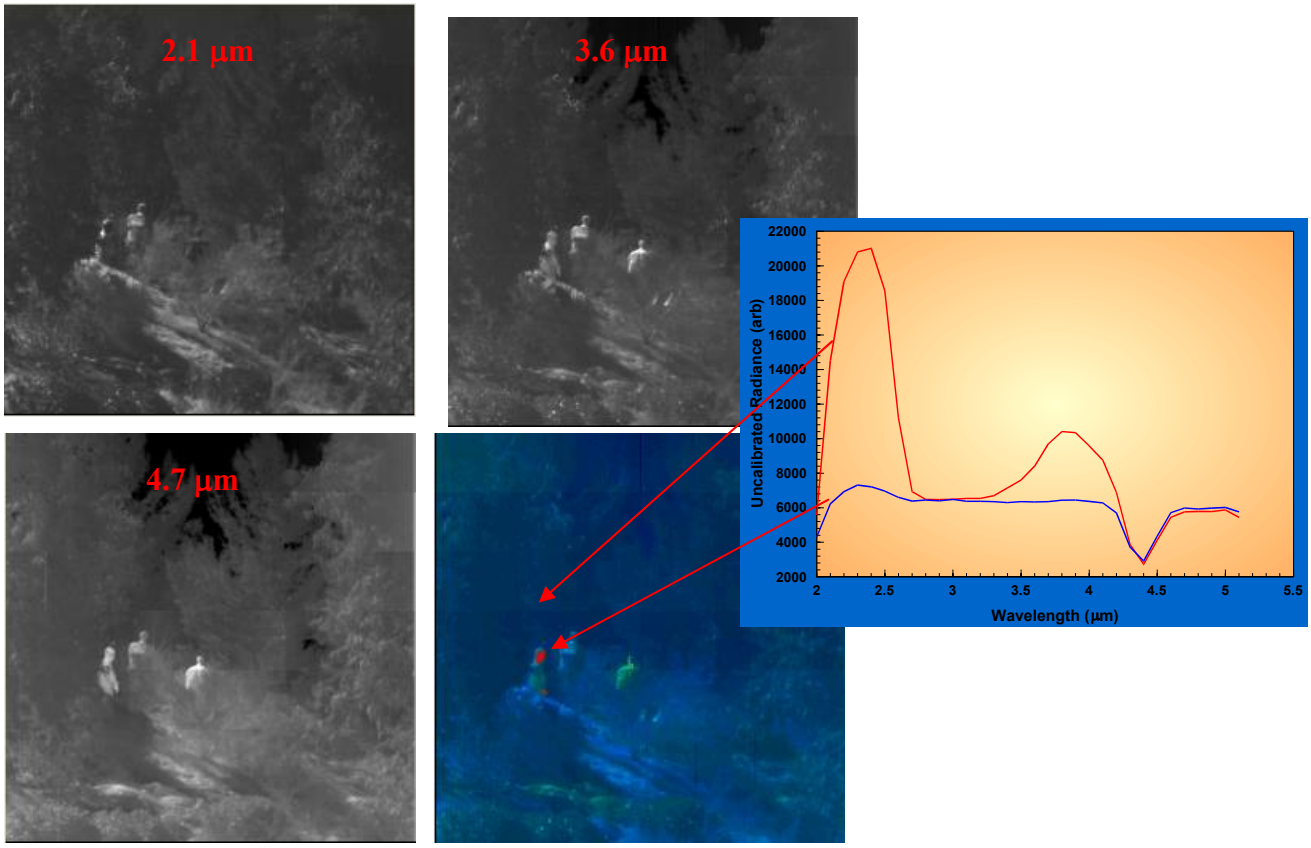

Figure 18: Skin's unique spectral reflectance allows real-time tracking of personnel

The above figure shows a person with two manikins in a cluttered scene at 2.1 μm, 3.6 μm, and 4.7 μm. Note the dark appearance of skin at 2.1 μm on the person (left center). Although the manikins appear similar, spectral processing

clearly shows the person's skin, both on the face and the visible hand. Note that as this person walked through the scene, the processor showed his position in real-time. When he disappeared behind bushes, he was re-acquired as soon as he came out from behind them, since his spectral signature did not change.

6. SUMMARY

In summary, a design for a real-time SWIR/MWIR hyperspectral imager has been described. Some of the optical and opto-mechanical design challenges have been detailed. A novel technique for mounting a prism assembly has been analyzed and optical performance data has been presented. Finally, hyperspectral data from the system has been collected. The results demonstrate the high performance of the system, spatially, spectrally, and temporally.

7. REFERENCES

1. M. Dombrowski, J. Bajaj, and P. Willson, "Video-rate Visible to LWIR Hyperspectral Imaging and Image Exploitation," 31st Applied Imagery Pattern Recognition Workshop, October 2002.
2. M. Dombrowski, , P. Willson and C. LaBaw, "Performance and Application of Real-Time Hyperspectral Imaging," SPIE Imaging Spectrometry IV, Vol 3438, July 1998.
3. B. Catanzaro, M. Dombrowski, , P. Willson, J. Hendrixson, E. Hillenbrand and J. Wilcox, "Manufacturing and Performance Evaluation of a Refractive Real-Time MWIR Hyperspectral Imager," SPIE Infrared Technology and Applications XXIX, Vol 5074, April 2003.